ADVANCED PHOTONICS RESEARCH
Open Access
www.adpr-journal.com

Implantable Nongenetic Optoelectronic Biointerfaces for Neuromodulation

Jinglin Ye, Jinwei Huang, Wenyu Nie, Jianming Xu, Xing Sheng, and Huachun Wang**

Electroceuticals are a novel type of therapeutics that employ electrical stimulation to modulate neural circuits and recover impaired physiological functions. Traditional systems using implanted leads as electrode and/or connecting wires pose several clinical challenges, including infection risk, anatomical incompatibilities, and leads dislodgement. Recent progress in optoelectronic biointerfaces is establishing new paradigms for electroceutical intervention by enabling precise, minimally invasive, and nongenetic neuromodulation through light-driven wireless technologies. In this review, first, the modulation mechanism of representative organic and inorganic semiconductor-based optoelectronic biointerfaces is demonstrated, which can be designed into flexible and tissue-conforming architectures. Then, further their capabilities to modulate structures at various levels, including neurons, nerve tissues, and the cerebral cortex are emphasized. Beyond neuromodulation, their promising therapeutic value and translational potential are highlighted, encompassing vision restoration, nerve regeneration, and treatment of Parkinson's disease. Together, these advancements mark a transformative shift toward next-generation bioelectronic medicine.

1. Introduction

The nervous system serves as the primary control center of the body. It employs intricate neural circuits to integrate sensory input and cognitive processes, facilitating adaptive responses essential for human existence.[1–3] More than one billion people around the world suffer from neurological problems such as neurodegenerative diseases, chronic pain, nerve injuries, and depression, presenting considerable social and economic challenges.[4,5] Electroceuticals, employing externally controlled electrical stimulation, have emerged as a transformative strategy in neuromodulation and neurotherapeutics, enabling targeted modulation of neural cells, fibers, neurotransmitter systems, and control circuits.[6] Electrostimulation modulates neuronal activity via complex interactions at the cellular and molecular levels. It works through three principal mechanisms: 1) initiation of action potentials occurs when charge transfer leads to membrane polarization beyond the threshold potential; 2) frequency-sensitive modulation of axonal conduction, influenced by myelin capacitance and nodal sodium channel kinetics; and 3) calcium-triggered synaptic plasticity via calcineurin activation and receptor trafficking.[7–15] By selectively repairing dysfunctional neural networks without compromising physiological signaling integrity, electroceuticals can modulate neural circuits with sub-millisecond precision.

Conventional electroceuticals deliver electrical stimulation to specific neural targets via wire-connected bioelectronic interfaces. Representative clinical applications include deep brain stimulation for tremor suppression in Parkinson's disease,[16,17] spinal cord stimulation for chronic pain management,[18,19] and transcutaneous vagus nerve stimulation for addressing epilepsy.[20,21] Despite their therapeutic efficacy, these lead-based systems present substantial clinical challenges, such as risks of infection, anatomical constraints, and lead displacement, particularly in pediatric populations. Additionally, reliance on battery-operated equipment compromises long-term therapy results by requiring frequent surgical procedures.[22–30] Optoelectronics integrates optics and electronics to create devices that transform photon energy into electricity or vice versa.[31,32] Optoelectronic biointerfaces that combine optoelectronic components with biological systems have been investigated as versatile tools for sensing, imaging, and stimulation in biomedical engineering.[33–36] Recent advances highlight their potential for neuromodulation by converting light into electrical signals that directly stimulate cells and tissues. Unlike conventional electroceuticals depending on wired electrodes, these light-driven systems provide wireless neural modulation with high

J. Ye, J. Huang, W. Nie, J. Xu, H. Wang
School of Integrated Circuits
Shenzhen Campus of Sun Yat-sen University
Shenzhen 518107, P. R. China
E-mail: wanghch36@mail.sysu.edu.cn

X. Sheng
Department of Electronic Engineering
Beijing National Research Center for Information Science and Technology, Institute for Precision Medicine
State Key Laboratory of Flexible Electronics Technology, and IDG/McGovern Institute for Brain Research
Tsinghua University
Beijing 100084, P. R. China
E-mail: xingsheng@tsinghua.edu.cn

The ORCID identification number(s) for the author(s) of this article can be found under https://doi.org/10.1002/adpr.202500176.

DOI: 10.1002/adpr.202500176

spatiotemporal precision, overcoming key limitations of traditional electrode-based approaches. Notably, optogenetics is another well-researched light-based neuromodulation method that relies on the genetic introduction of light-sensitive ion channels into target cells.[37–40] The genetic modification poses ethical and translational challenges. Regarding of this issue, optoelectronic modulation provides a practical, nongenetic alternative that preserves the advantages of optogenetics while avoiding ethical controversies and reducing complexity.

Semiconductor materials, characterized by their highly tunable physical properties, are fundamental to the advancement of optoelectronic based modulation platforms.[32,33,41] Recent progress in semiconductor technology has significantly accelerated the development of optoelectronic biointerfaces, facilitating neuromodulation across diverse scales.[42–44] In this review, we first elucidate the mechanism of signal transduction at semiconductor-based optoelectronic biointerfaces and summarize representative organic and inorganic semiconductor materials and devices. To satisfy different application needs, these semiconductors could be engineered into various flexible architectures, such as nanorod arrays, quantum dots (QDs), thin films, and mesh structures. The mechanically soft designs provide intimate, conformal touch with delicate neural tissue. To elucidate the mechanisms underlying neural modulation, we then detail the functionality of semiconductor-based optoelectronic biointerfaces in modulating neurons, peripheral nerves, and the cerebral cortex. We finally highlight their expanding therapeutic applications and clinical potential, including their roles as nerve conduits for regeneration, retinal prostheses for vision restoration, and opto-electrodes for treating neurological disorders such as Parkinson's disease. This review concludes by summarizing recent advances, discussing key challenges, and future directions in optoelectronic neural interface research.

2. Mechanism and Semiconductor Materials for Optoelectronic Biointerfaces

The modulation capability of optoelectronic biointerfaces stems from the ability of semiconductors to convert light into electrical or electrochemical signals in complex biological aqueous microenvironment containing water and electrolytes. As shown in **Figure 1**a, the light-to-electricity conversion in semiconductors primarily occurs through three main types of homojunctions and heterojunctions. Despite differences in energy band structure, the underlying mechanisms are fundamentally similar. Upon absorption of incident photons, electrons in the semiconductor are excited to higher energy states, leaving behind holes in the valence band. These photogenerated electron–hole pairs are driven toward the semiconductor surface by the built-in electric field established at the homojunction or heterojunction interface. As charge carriers (e.g., electrons) accumulating near the semiconductor-solution interface, oppositely charged ions (e.g., cations) in the biological solution are attracted to the interface, forming electric double layer and generating a transient charging capacitive current.[45] If charge carriers are injected into solution, this occurs via redox reactions, typically involving neutral species like dissolved oxygen or water, leading to sustained

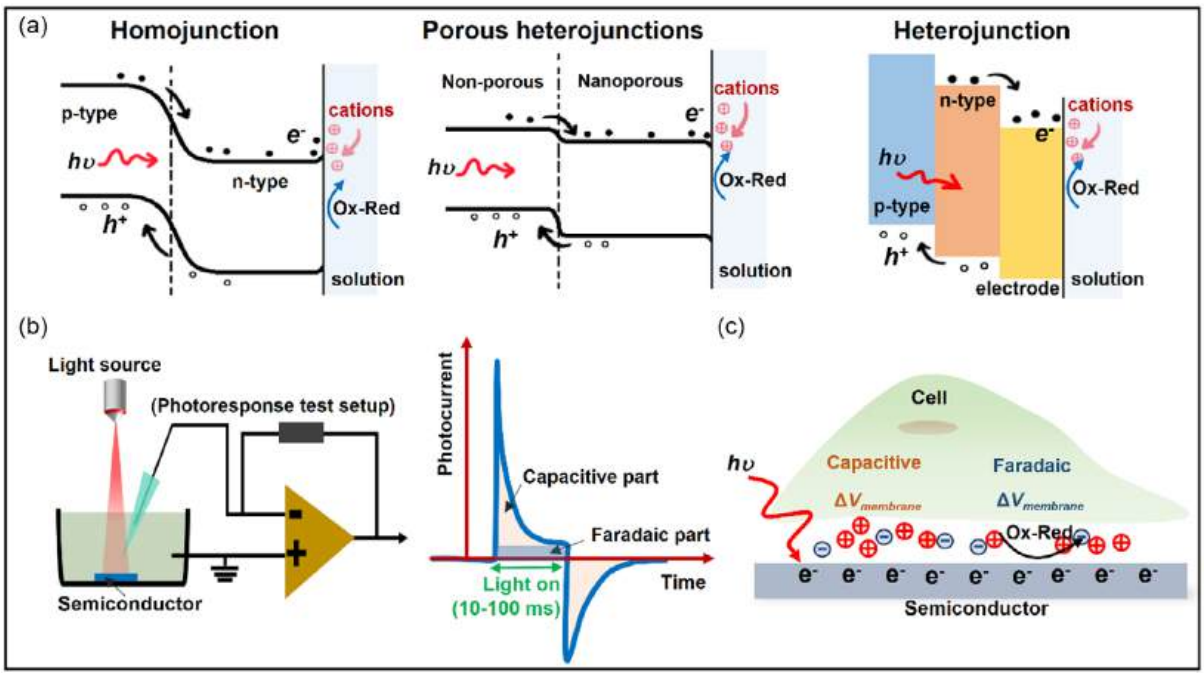

Figure 1. Diagrams of modulation mechanism for optoelectronic biointerfaces. a) Band structures of different semiconductor junctions used in constructing optoelectronic biointerfaces. b) Schematics of the photoresponse measurements setup for optoelectronic biointerfaces (left) and the two major response types, the capacitive and the Faradaic (right). c) Illustration of membrane potential changes driven by light-induced faradaic and capacitive charge transfer mechanisms.

Faradaic current.[32] The capacitive biointerfaces generally exhibit superior stability and reversibility compared to the Faradaic counterparts, as their operation avoids electrochemical reactions. Consequently, the electrochemical water window is a key constraint for design of long-term stable optoelectronic biointerfaces. It defines the potential range within which water remains electrochemically inert, thereby preventing Faradaic reactions such as electrolysis and gas evolution.[46] Actually, this window depends on multiple factors, including the semiconductor's bandgap, Fermi level, band edge alignment, surface states (e.g., defects or metallic modification), and electrolyte compositions. The bandgap and Fermi level offset primarily determine the photovoltage that a semiconductor can generate under illumination. When this photovoltage exceeds 1.23 V (theoretical potential for water splitting), water electrolysis will occur.[47] Band edge alignment refers to the positioning of a semiconductor's conduction band minimum and valence band maximum relative to the redox potentials of chemical species in solution (e.g., O_2/H_2O, H^+/H_2). The alignment dictates whether photogenerated electrons or holes have enough energy to drive reduction or oxidation reactions.[48] Surface states also play a significant role in modulating interfacial charge transfer. For example, Jiang et al. demonstrated that noble metal Au (gold) or Pt (platinum) decoration of silicon significantly enhanced Faradaic currents by lowering activation barriers.[49] Additionally, a recent study highlighted the definition of water window is strongly influenced by electrolyte composition, with phosphate-buffered saline (PBS) producing different electrochemical responses compared to culture media.[50] The capacitive and Faradaic processes induced by light at the biointerface (namely, optoelectronic biointerface) can be characterized using electrochemical measurement systems and/or patch-clamp techniques. The electrochemical techniques based on three and/or two-electrode setups such as cyclic voltammetry, chronoamperometry, and electrochemical impedance spectroscopy are widely used to characterize the electrochemical properties of traditional wired electrodes.[10,51,52] These methods allow quantitative assessment of charge transfer, interfacial impedance, and the distinction between capacitive and Faradaic processes. While optoelectronic biointerfaces operate wirelessly, electrochemical measurements are still essential for probing interfacial charge dynamics, drawing on approaches established in semiconductor photocatalysis and photoelectrocatalysis. Recently, patch-clamp systems (widely used in electrophysiology) have been adapted to evaluate the wireless photoresponse of optoelectronic interfaces in vitro. As shown in Figure 1b (left), a glass micropipette electrode (1–10 MΩ) is positioned closely (≈2 μm) to the semiconductor surface in electrolyte (e.g., PBS). Controlled light pulses from a laser or LED are delivered via an optical fiber or microscope objective, and the resulting photocurrent or photovoltage at the semiconductor–electrolyte interface is recorded in real time. This configuration provides high spatiotemporal resolution recordings of subtle ionic dynamics at the biointerface, particularly in wireless optoelectronic devices under physiologically relevant conditions.[49,53] A typical photocurrent trace captured by patch-clamp system shown in Figure 1b (right),it can be decoupled into capacitive and Faradaic components. The capacitive current exhibits upward and downward transient spikes, corresponding to the charging and discharging processes, respectively. In contrast, the Faradaic current appears as a sustained (during illumination), low-amplitude signal, indicating redox reactions at the interface. In both scenarios, the current changes the local electric potential in cellular microenvironment. Neurons, as excitable cells, are particularly sensitive to these changes and respond by adjusting their membrane potential (Figure 1c). Briefly, the operational principle of optoelectronic neuromodulation is governed by two synergistic mechanisms: 1) the photoelectric response of semiconductors and 2) the electrophysiological sensitivity of neurons to externally generated electrical signals. Unlike conventional electrical stimulation techniques, this approach allows for wireless and nongenetic modulation of neural activity. Modifying key optical parameters (illumination intensity, pulse duration, frequency, and spot area) enables precise, spatiotemporally controlled neural stimulation via programmable light inputs.

Building on these principles, the efficacy of optoelectronic neuromodulation is fundamentally dependent on the photoconversion efficiency and stability of the biointerface, both of which are crucial for dependable neural modulation. Extensive investigations have been conducted on a wide range of semiconductor systems. **Table 1** summarizes the representative materials currently employed in optoelectronic biointerfaces. The design of materials and devices for neural optoelectronic interfaces must consider several key criteria. First, a suitable bandgap is crucial, especially for fully implantable devices. Leveraging the optical transparency window of biological tissue simplifies light delivery, minimizes invasiveness, and enables efficient wireless operation. Four optical biological windows defined in biomedical optics: near-infrared (NIR)-I (650–950 nm), NIR-II (1000–1350 nm), NIR-III (1600–1870 nm), and NIR-IV (2100–2300 nm).[54] NIR-I and NIR-II are preferred, providing sufficient tissue penetration and alignment with the bandgaps of commonly used semiconductor materials. In contrast, light in the NIR-III and NIR-IV ranges is more strongly absorbed by water, leading to increased thermal effects that may impair neural viability.[55] To minimize thermal damage, irradiance should comply with established safety thresholds, such as those set by ANSI Z136.1 and ICNIRP, which define maximum permissible exposure based on wavelength, exposure time, and tissue properties.[56,57] Adhering to these limits and guidelines is essential for safe and effective in vivo neuromodulation. Second, scalable, cost-efficient fabrication methods, along with high processability of materials are important for practical application. For example, high material processability allows the creation of diverse architectures (e.g., nanorod arrays, QDs, thin films, and mesh structures), tailored for specific applications. It can also improve mechanical compatibility via structurally soft and flexible design, thereby reducing immune responses and promoting long-term neural interface stability.[58] Last but not the least, material stability and biocompatibility are critical factors to consider. The stability requirements differ by application: transient electronic devices are intended to biodegrade after a defined period, while chronic implants demand highly stable and corrosion-resistant optoelectronic interfaces. Notwithstanding this, biocompatibility is essential in every instance. However, extensive, longitudinal assessments of biosafety and biocompatibility are still few and necessitate additional advancement.[43]

Table 1. Representative semiconductor materials used in optoelectronic biointerfaces.

Category	Materials	Structures	Applications	Ref.
Inorganic semiconductors	Si[a)]	Nanowires, thin film, nanoporous	Neuron/nerve/cortex modulation, vision restoration, nerve regeneration	[62,81,87,95,109–114]
	Te[b)]	Nanowires	Vision restoration	[89,90]
	TiO_2/TiO_x[c)]	Nanowires, nanorods		[89,90]
	$FAPbI_3$,[d)] $CsPbI_3$[e)]	Nanowires array		[93]
	HgTe[f)], InP[g)], ZnS[h)], AlSb[i)], PbS[j)], CdS[k)], $AgBiS_2$[l)]	QD, thin film	Neuron modulation	[63,64,115–123]
	NUNCD[m)]	Thin film	Neuron modulation	[124]
Organic semiconductor	PTCDI[n)]-H_2Pc[o)]	Thin film	Neuron and nerve modulation	[66,71,82,125,126]
	ZnTPyP[p)]	Nanorods	Neuron modulation and treatment of Parkinson's disease	[96]
	P3HT[q)]-PCBM[r)]	Thin film	Neuron modulation and vision restoration	[88,127–130]

[a)]Si: silicon [b)]Te: tellurium [c)]TiO_2/TiO_x: titanium oxide [d)]$FAPbI_3$: formamidinium lead iodide [e)]$CsPbI_3$: cesium lead triiodide [f)]HgTe: mercury telluride [g)]InP: indium phosphide [h)]ZnS: zinc sulfide [i)]AlSb: aluminum antimonide [j)]PbS: lead sulfide [k)]CdS: cadmium sulfide [l)]$AgBiS_2$: silver bismuth sulfide [m)]NUNCD: nitrogen-doped ultrananocrystalline diamond [n)]PTCDI: N,N′-dimethylperylene 3,4,9,10-tetracarbon diimide [o)]H_2Pc: phthalocyanine [p)]ZnTPyP: zinc porphyrin [q)]P3HT: poly-3-hexylthiophene [r)]PCBM: [6,6]-phenyl-C61-butyric acid methyl ester.

3. Optoelectronic Biointerfaces for Neuronal Modulation

Neurons are the basic units of the nervous system. Under normal conditions, neurons transmit signals via alterations in membrane potential and ions flow, facilitating the communication and coordination essential for many physiological tasks.[59,60] However, abnormal neuronal electrical activity can disrupt this delicate balance, potentially leading to various neurological disorders. In this context, optoelectronic modulation devices offer the capability to regulate neuronal activity by generating localized electrical stimulation in response to light cues. The goal of this technique is to activate, inhibit, or modify the electrophysiological activity of neurons, which is fundamental to neuromodulation and neural therapeutics.

Recent researches have explored the ability of various semiconductor materials to modulate cellular activity. Gao et al. proposed an injectable magnetically manipulated optoelectronic hybrid micro-robot (MOHR) for optically targeted nongenetic neuromodulation.[61] The integration of magnetic components enables targeting with high precision. As shown in **Figure 2**a, the MOHR was fabricated with a core-shell nanowire metal-insulator–semiconductor (MIS)structure, exhibiting a rod-like geometry. The results demonstrated changes in hippocampal neuronal membrane potential in an Aβ42-induced Alzheimer's disease (AD) model, before and after light-driven electrical stimulation (532 nm. 10 ms pulse duration, powers of 530 mW cm^{-2}, photocurrent ≈ 75 nA) via internalized MOHR, confirming its targeted optical neuromodulation capability and its potential for Alzheimer's disease treatment. The biocompatibility of MOHR was further evaluated using a nonradioactive colorimetric assay. After 48 h of exposure, no significant reduction in cell viability was observed at concentrations ≤ 16 μg mL^{-1} for Si and MOHR, indicating their low cytotoxicity and favorable biocompatibility.

The junction-type thin-film structure is a typical structure utilized in biointerfaces for cellular optoelectronic modulation. Figure 2b shows that the study provided a thin-film single-crystal silicon-based *p*-n diode that selectively produces photo-induced electrical signals for deterministic neuromodulation.[62] The activation or inhibition of neuronal activity depends on the ability of different types of junctions (p^+n and n^+p type Si) to attract or reject charged particles. The right picture in Figure 2b shows the membrane potential recordings from rat dorsal root ganglion neurons when they were exposed to different types of thin-film diodes. The p^+n type Si film generated a photovoltage of −30 to −60 mV, increasing membrane potential and inducing depolarization. In contrast, the n^+p type Si film produced a photovoltage of +30 to +60 mV, decreasing membrane potential and leading to hyperpolarization. This study exploited photoelectric modulation to achieve wireless, nongenetic, and bidirectional control of neural cells.

Alongside conventional silicon-based semiconductors, QD materials derived from lead sulfide (PbS) mercury telluride (HgTe), cadmium selenide (CdSe), indium phosphide (InP), and aluminum antimony (AlSb) have been investigated. QDs are extremely small semiconductor materials, typically ranging from a few to tens of nanometers in size. QDs display quantum mechanical phenomena, particularly the quantum confinement effect, as their dimensions are equivalent to or lower than the Bohr radius of the material. These "zero-dimensional" nanostructures restrict electrons and holes, resulting in discrete energy levels and imparting QDs with unique optoelectronic capabilities that differ from bulk materials. A flexible PbS QDs-based optoelectronic biointerface was developed to activate cells using near-infrared light ($\lambda = 780$ nm) within the spectral

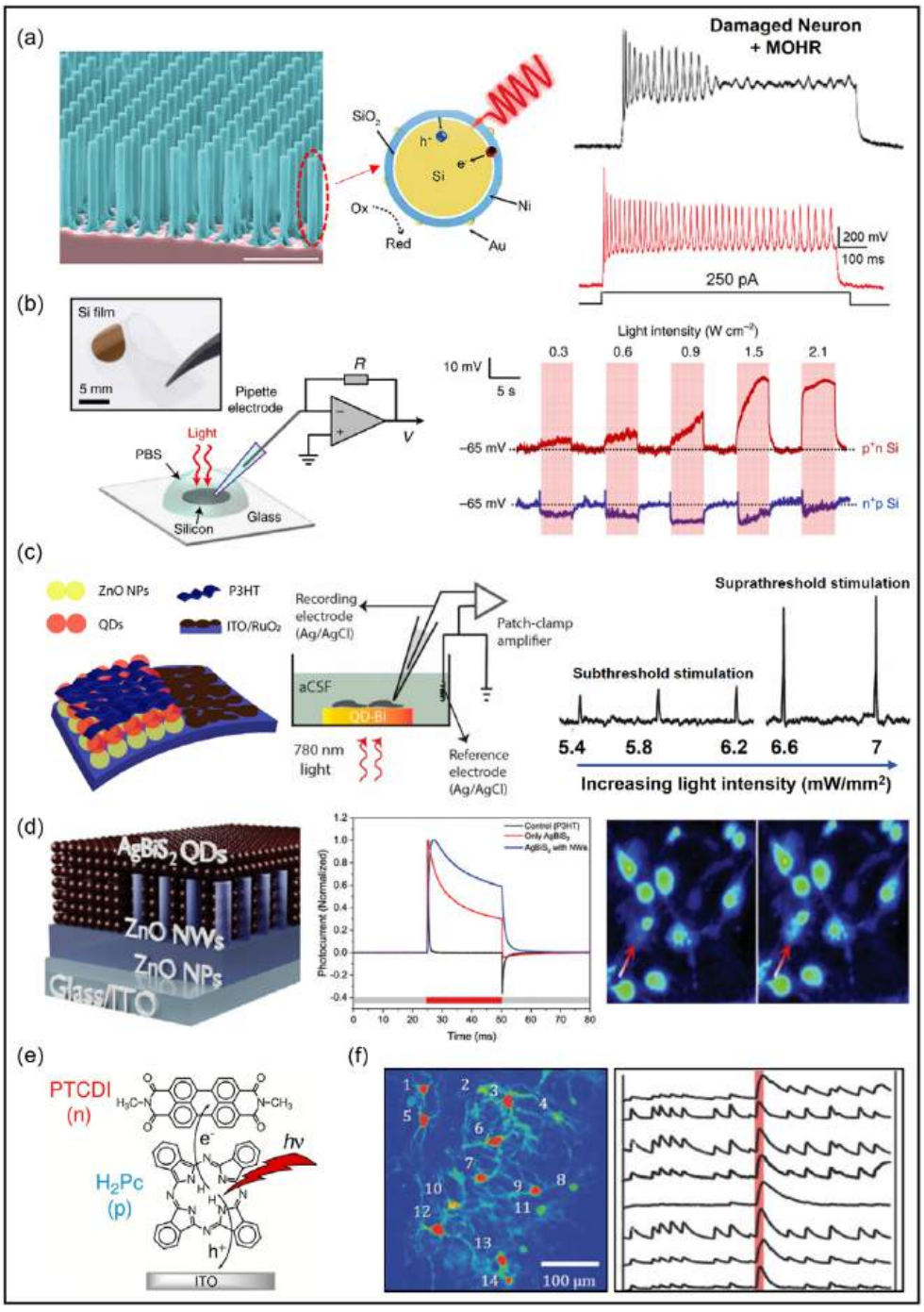

Figure 2. Optoelectronic biointerfaces for neuronal modulation. a) Magnetically manipulated optoelectronic hybrid microrobots for neuromodulation. Scanning electron microscopy images of MIS nanowires array grown on the silicon substrate (left). Representative membrane potential recordings of a hippocampal neuron with internalized MOHRs incubated with 2 μm oligomeric Aβ42 for 1 h, before and after laser illumination. Reproduced with permission.[61] Copyright 2024, Wiley-VCH. b) Scheme of the setup for the photoresponse measurement (left) and typical traces from current-clamp recordings of the dynamic depolarized and hyperpolarized membrane voltages generated by differently polarized photoelectric fields during a train of varying light intensities (right). Reproduced with permission.[62] Copyright 2023, Springer Nature. c) Schematic of the multilayered biointerface architecture (left) and simplified schematic of intracellular recording setup using patch-clamp amplifier (middle), current-clamp recordings of hippocampal neurons under increased light intensity (right). Reproduced with permission.[63] Copyright 2022, ACS Publications. d) Schematic of the ZnO-$AgBiS_2$ QDs-based pseudocapacitive device (left), photocurrent characteristics of the $AgBiS_2$-NW-based device (middle), rainbow-colored calcium imaging of a single neuron cultured on the device following 780 nm light stimulation (5 Hz, 20 ms). Reproduced with permission.[64] Copyright 2025, Wiley-VCH. e) Structure of organic photocapacitors. Reproduced under terms of the CC-BY license.[65] Copyright 2019, The Authors. American Association for the Advancement of Science. f) Cortical primary neurons cultured on type I devices and Ca^{2+} imaging traces. Reproduced with permission.[66] Copyright 2018, Wiley-VCH.

tissue transparency window. The integration of a 25 nm ultrathin QD layer into a multilayered photovoltaic structure enabled the conversion of near-infrared light into safe capacitive ionic currents, reliably eliciting action potentials in primary hippocampal neurons. This platform delivered over 5 μC cm^{-2} of charge during 20 ms pulses at a light intensity of 1 mW mm^{-2}—within the threshold range for stimulating neural structures such as the optic nerve, auditory nerve, and subthalamic nucleus (Figure 2c).[63] Although this investigation revealed that the system has little biotoxicity, its stable photoelectric response characteristics suggest great potential for applications in neural modulation and the treatment of neurological diseases. Recently, Balamur et al. developed an optoelectronic biointerface based on $AgBiS_2$ (silver bismuth sulfide) QDs integrated with zinc oxide nanowires (Figure 2d left). In this system, $AgBiS_2$ QDs function as the photoabsorber, hole transport medium, and pseudocapacitive electrode–electrolyte interface, effectively enhancing the device's photoelectrochemical response (Figure 2d middle). Notably, $AgBiS_2$ is free of lead and other heavy metals, offering improved biosafety and biocompatibility. Upon pulsed 780 nm illumination, the device could produce a charge injection density of ≈29 μC cm^{-2}, and effectively triggered intracellular calcium release (Figure 2d right), demonstrating its potential for safe and efficient neuronal photostimulation.[64]

Research on neural stimulation utilizing organic semiconductors reveals a viable approach that incorporates PTCDI as an n-type material and H_2Pc as a p-type material to fabricate organic electrolytic photocapacitors (OEPCs), as shown in Figure 2e.[65] These devices could generate sufficient localized capacitive currents under light exposure to stimulate neurons. Figure 2f presents calcium imaging traces of primary neurons cultured on samples (chromium/gold/H_2Pc/PTCDI) under illumination (600 nm, 480 mW cm^{-2}, 5 ms, photovoltage ≈40 mV),[66] demonstrating the potential of organic photocapacitor for effective neuromodulation.

Table 2 summarizes the key parameters (wavelength, pulse duration, frequency, and power) used in optoelectronic biointerfaces for neuronal modulation, enabling comparison across in vivo and ex vivo studies. These examples demonstrate that optoelectronic biointerfaces can deliver spatially confined electrical stimulation to neuronal cells at the microscale, allowing precise modulation of cellular activity without genetic modification. As a lead-free platform, they serve as a valuable tool for investigating the effects of electrical stimulation. Beyond their experimental role, these systems can deepen our understanding of the mechanisms underlying neurological disorders.

Table 2. Key parameters for neuronal modulation.

Wavelength [nm]	Pulse duration [ms]	Power density [mW cm^{-2}]	Frequency [Hz]	Photocurrent/ photovoltage	Ref.
532	10	530	–	≈20 [nA]	[61]
635	5000	1800	–	≈70 [mV]	[62]
780	10	500	80	≈7 [nA]	[63]
780	20	58	5	≈1.9 [mA · cm^{-2}]	[64]
630	20	600	1.75	≈670 [μA · cm^{-2}]	[65]
600	5	480	67	≈40 [mV]	[66]

4. Optoelectronic Biointerfaces for Brain Modulation

The brain serves as the body's command center, regulating everything from movement and sensory perception to memory and emotion. It communicates with the rest of the body via the central nervous system. The outer layer, the cerebral cortex, is critical for higher cognitive functions such as reasoning, decision-making, and language.[67–69] Recent studies have investigated optoelectronic biointerfaces for modulating cortical activity, showing promise for treating neurological disorders such as Parkinson's disease, epilepsy, and depression.

Jiang et al. developed a flexible membrane composed of a gold-decorated p-i-n silicon mesh integrated with a porous PDMS (polydimethylsiloxane) substrate to interface with the mouse brain cortex for neural modulation (**Figure 3**a).[49] This device conforms well to the cortical surface, ensuring strong adhesion. Photoelectric stimulation via an extracellular linear array placed on the cortical surface showed significant enhancement of neural activity in response to light exposure (473 nm, ≈5 mW, 100 ms, ≈216 μm spot size). Notably, the device also induced specific limb movements in anesthetized mice, highlighting its potential for precise neural control. Building on this, Huang et al. demonstrated that p^+n junction thin-film silicon diodes could robustly activate superficial neurons, while n^+p configurations could effectively suppress pre-existing cortical activity under illumination (Figure 3b).[62] This demonstrated the bidirectional regulation capability of the junction-type thin-film silicon diodes for cortical neural activity.

Organic semiconductor junctions such as PTCDI/H_2Pc have been also used for cortical stimulation in mice. Missey et al. implanted PTCDI/H_2Pc-based OEPC on the cortical surface and activated it with deep red light (638 nm, 5 ms pulses at a 33 mW cm^{-2}, photocurrent 1.5 mA cm^{-2}), evoking electrophysiological responses and visible whisker movements without removing skin or skull (Figure 3c).[70] Although responses attenuated over time due to the delamination either between the device and neural tissue or among internal functional layers of the device, the approach enabled noninvasive motor cortex activation. Nowakowska et al. extended this work by stimulating multiple brain regions, somatosensory cortex, entorhinal cortex, and hippocampus (Figure 3d).[71] Statistical analysis of c-Fos positive neurons revealed a significant increase in expression across all examined regions, indicating that OEPC stimulation induces widespread neuronal activation during brain tissue modulation.

Optoelectronic biointerfaces enable wireless, flexible, and bidirectional control of cortical activity, offering potential therapies for disorders such as depression, epilepsy, and Parkinson's disease. However, clinical translation faces major challenges due to the thicker human scalp and skull, and the need for long-term treatments. Limited light penetration and device stability remain key obstacles. Progress requires tuning stimulation wavelength within the 650–950 nm biological window to enhance tissue penetration, and alongside improving conversion efficiency (e.g., via semiconductor bandgap engineering). Durable and

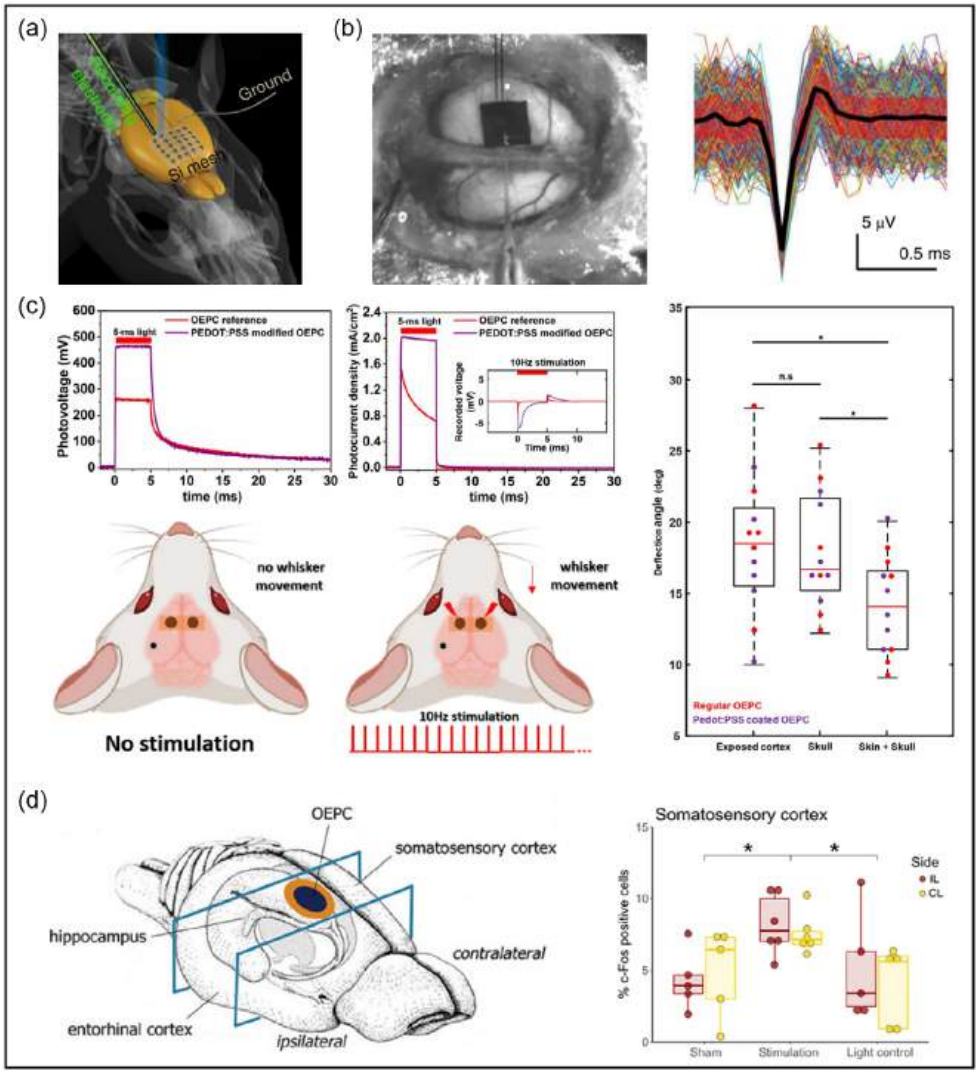

Figure 3. Optoelectronic biointerfaces for brain modulation. a) Schematic diagram of in vivo optoelectronic stimulation testing on the intact mouse somatosensory cortex with a silicon mesh attached. Reproduced with permission.[49] Copyright 2018, Springer Nature. b) Thin-film silicon diodes installed on the mouse cortical surface (left) and typical extracellular electrophysiological recordings of spike events in response to stimulation (right). Reproduced with permission.[62] Copyright 2023, Springer Nature. c) Photoresponse performance and schematic diagram of whisker deflection induced by OEPC (left), applied light to the exposed cortex, stimulating the whisker deflection angle recorded through the skull or by penetrating both the skin and skull (right). Reproduced with permission.[70] Copyright 2021, IOP Publishing Ltd. d) Illustration of the placement of OEPC (orange-deep blue circles) and the section sampled (blue rectangle between) (left) along with the percentage of c-Fos$^+$ cells in the somatosensory cortex (right). Reproduced under terms of the CC-BY license.[71] Copyright 2024, The Authors, Wiley-VCH.

biocompatible encapsulation materials, such as PDMS, parylene, and silicon dioxide, are also essential to maintain long-term performance and safety.

5. Optoelectronic Biointerfaces for Peripheral and Vagus Nerves Modulation

The peripheral nervous system (PNS) links the brain and spinal cord to peripheral organs, enabling the central nervous system to monitor internal and external environments and regulate vital physiological functions.[72] As a key component of the PNS, the vagus nerve modulates cardiovascular, gastrointestinal, pulmonary, and immune functions, influencing heart rate (HR), digestion, and inflammatory responses.[73,74] Neuromodulation of peripheral and vagal nerves holds therapeutic potential in pain relief, restoration of motor and visceral function, and treatment of psychiatric disorders.[75–78] Clinically, left-sided vagus nerve stimulation (VNS) is approved for refractory epilepsy and depression, while right-sided VNS has shown benefit in heart failure in both preclinical and clinical studies.[79,80] Recent advances in optoelectronic biointerfaces for vagal and peripheral nerve stimulation highlight the potential of light-based, minimally invasive approaches for next-generation neuromodulation therapies.

Thin-film silicon diodes, as previously described, can also be applied to peripheral nerve modulation (**Figure 4**a).[62] After being transferred onto flexible polyethylene terephthalate (PET) substrates, these devices could conform to the surface of exposed sciatic nerves in mice. Illumination with 635 nm laser light (0.04–1.8 W cm^{-2}) induced compound muscle action potentials (CMAPs) and hindlimb movement through photonic activation of p^+n type silicon-based optoelectronic biointerfaces. These interfaces generated a positive potential (+30 to +60 mV), sufficient to depolarize nerve fibers and trigger motor responses. In contrast, n^+p type silicon-based optoelectronic biointerfaces failed to elicit motor activity under identical conditions, as the resulting negative potential (−30 to −60 mV) inhibited nerve signal propagation and suppressed CMAP generation. Prominski et al. developed a nanostructured porous/nonporous silicon heterojunction via stain etching (Figure 4b).[81] Compared to conventional p–n junctions in Si, nanoporous/nonporous heterojunctions achieve diode-like behavior without the need for complex doping process. The increased surface area and antireflective properties of the nanoporous structure improved light absorption and overall photoelectrochemical performance. After an oxygen plasma treatment, the nanoporous Si film could obtain a charge injection of ≈0.25 nC under 532 nm light irradiation (pulse duration 10 ms, ≈4.3 W cm^{-2}). Moreover, the porous surface offers enhanced mechanical compliance, facilitating seamless integration with soft biological tissue. By varying 808 nm laser power (15, 112, and 209 mW mm^{-2}), the study achieved muscle activation selectively, reflecting differential thresholds within the nerve bundle, which provides a strategy to enhance specificity and minimize discomfort in clinical applications.

Organic semiconductors have also shown advancing potential in peripheral nerve modulation. Ejneby et al.[82] and Donahue et al.[83] applied OEPC and organic photovoltaics for sciatic nerve stimulation in rats (Figure 4c) and vagus nerve stimulation in mice (Figure 4e), respectively. In the former, the OEPC yields a photoinduced charge density exceeding 1.25 μC cm^{-2} under 638 nm illumination with a 1 ms pulse. Chronic stimulation using a 638 nm laser at 700 mW over three months elicited stable CMAPs for more than 60 d. A decline on day 77 was reversed by reducing tissue light attenuation, suggesting reduced efficacy was due to suboptimal excitation from device degradation rather than nerve damage. In the latter, right cervical vagus nerve stimulation, which is related to sinoatrial node regulation, induced a real-time reduction in HR. The vagus nerve's smaller size limited light absorption, weakening stimulation efficacy. To overcome this, the authors developed a "photovoltaic flag" device, relocating the light-harvesting area outside the nerve. This design achieved HR reductions > 5% in mice with moderate or normal stimulation thresholds.

In studies on various optoelectronic materials, Jakešová systematically investigated the impact of photovoltaic cell size, series configurations, and microelectrode coupling with various materials, outlining design principles for implantable photovoltaic nerve stimulators (Figure 4d).[84] In practical applications, stimulation currents are often limited by the electrode interface rather than the photovoltaic driver. To address this, the authors systematically compared eight commonly used neural interface electrodes: Ti, TiN (titanium nitride), Pt, Au, W (tungsten), IrO_x (iridium oxide), PEDOT:PSS (poly(3,4-ethylenedioxythiophene) poly(styrenesulfonate), and PtO_x (platinum oxide), representing capacitive, Faradaic, and pseudocapacitive charge injection mechanisms. PEDOT:PSS showed the lowest impedance, followed by IrO_x and nanoporous Pt (PtO_x). Charge injection capacity scaled with electrode surface area. Furthermore, photovoltaic cell configuration played a key role: series connections increased output voltage, favoring high-impedance or small-area electrodes, while parallel connections enhanced current delivery, benefiting low-resistance, large-area, or Faradaic systems. Simulations and experiments revealed a strong interdependence among electrode material, geometry, and photovoltaic configuration, highlighting the need for co-optimization to enable efficient and precise neural stimulation. Nongenetic optoelectronic biointerfaces have been validated in rodents for peripheral and vagus nerve stimulation, providing flexible, programmable, bidirectional, and stable electrophysiological modulation with therapeutic potential in pain management, motor disorders, and organ dysfunction. Key challenges include variable nerve size and depth across anatomical sites, requiring application-specific adaptation beyond considerations of stimulation intensity and tissue penetration. Notably, the larger nerve dimensions in humans and large animals may facilitate translation to clinical settings.

6. Optoelectronic Biointerfaces as Retinal Prosthesis for Vision Restoration

Retinal degeneration such as retinitis pigmentosa, is a major cause of irreversible blindness, primarily resulting from photoreceptor loss and consequent disruption of visual signal transmission.[85] Retinal prostheses have emerged as a promising strategy, electrically stimulating surviving retinal neurons to bypass degenerated photoreceptors (rods/cones) and convert optical input into electrophysiological signals interpretable by the brain.[86] These typical optoelectronic biointerfaces aim to directly activate residual neurons to reconstruct visual pathways.

Lorach et al. developed a hexagonal silicon array incorporating multistage series-connected photodiodes, as shown in **Figure 5**a.[87] Using localized electric field confinement, this design limits single-pixel activation to 70 μm and achieves a spatial resolution of 64 ± 11 μm in degenerate rats. In rodent models, the system restored up to 50% of normal visual acuity. Expanding visual field coverage is equally critical for optimizing visual prosthetic performance. Chenais et al. advanced this paradigm with a 10 498-unit photovoltaic implant featuring microscale pixels (diameter: 80 μm, 120 pitch: 120 μm) spanning 13.4 mm^2 of retinal surface (Figure 5b).[88] When exposed to 560 nm, light at 0.9 mW mm^{-2}, each pixel could produce a photovoltage of ≈30 μV. In the editing of retinal prostheses, it is particularly important to improve their response to different wavelengths of light. Tang et al. addressed this by developing a retinal prosthesis based on Au nanoparticle-decorated TiO_2 nanowire arrays, as shown in Figure 5c. This one-dimensional semiconductor nanowire array demonstrated multiwavelength photoresponse, including near-ultraviolet (375 nm, 133 μW mm^{-2}), blue (470 nm, 691 μW mm^{-2}), and green (546 nm, 470 μW mm^{-2}) light, with corresponding average photocurrent changes of ≈1450, 108, and 87 pA, respectively. Combining high spatial resolution

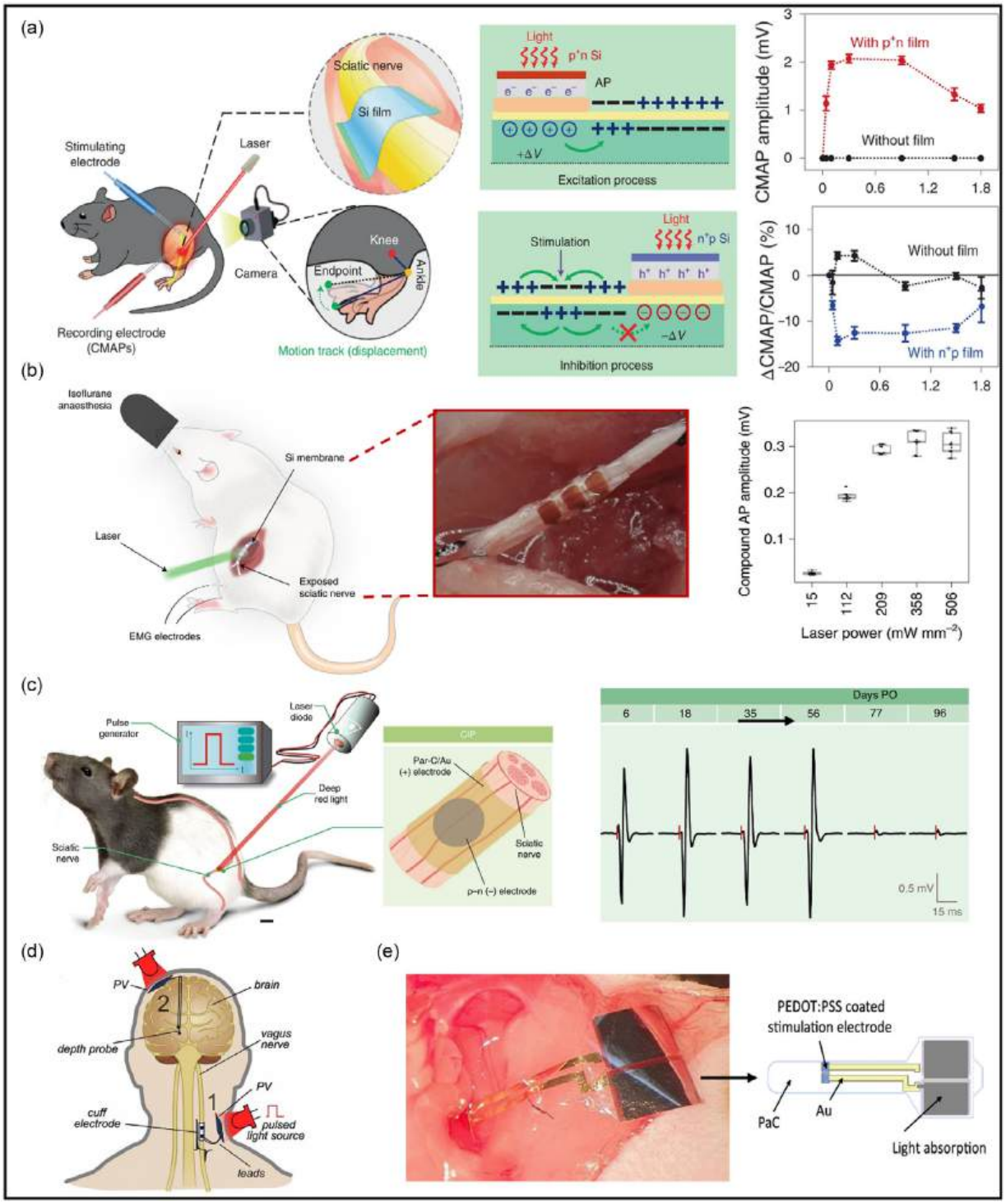

Figure 4. Optoelectronic biointerfaces for peripheral and vague nerves modulation. a) Schematic diagram of light irradiation on a silicon-based thin-film photodiode attached to the sciatic nerve, modulating mouse hindlimb movement (left), along with the principle of bidirectional neural modulation (middle) and the recorded CMAP amplitude (right). Reproduced with permission.[62] Copyright 2023, Springer Nature. b) Schematic diagram of sciatic nerve stimulation in an acute in vivo rat model using a porosity-based heterojunction, with the CMAP amplitude generated under a 808 nm NIR laser, 10 ms pulse. Reproduced with permission.[81] Copyright 2022, Springer Nature. c) Schematic diagram of in vivo optical stimulation of the sciatic nerve using an implanted OEPC (left) and representative average CMAP during a 103 d chronic implantation period (right). Reproduced with permission.[82] Copyright 2021, Springer Nature. d) Concept diagram of potential applications for an implantable photovoltaic-driven neural stimulator. Reproduced with permission.[84] Copyright 2024, IOP Publishing Ltd. e) Schematic diagram of a photovoltaic flag, with microelectrodes wrapped around the right vagus nerve and the photovoltaic flag placed above the salivary glands and skin. Reproduced with permission.[83] Copyright 2022, IOP Publishing Ltd.

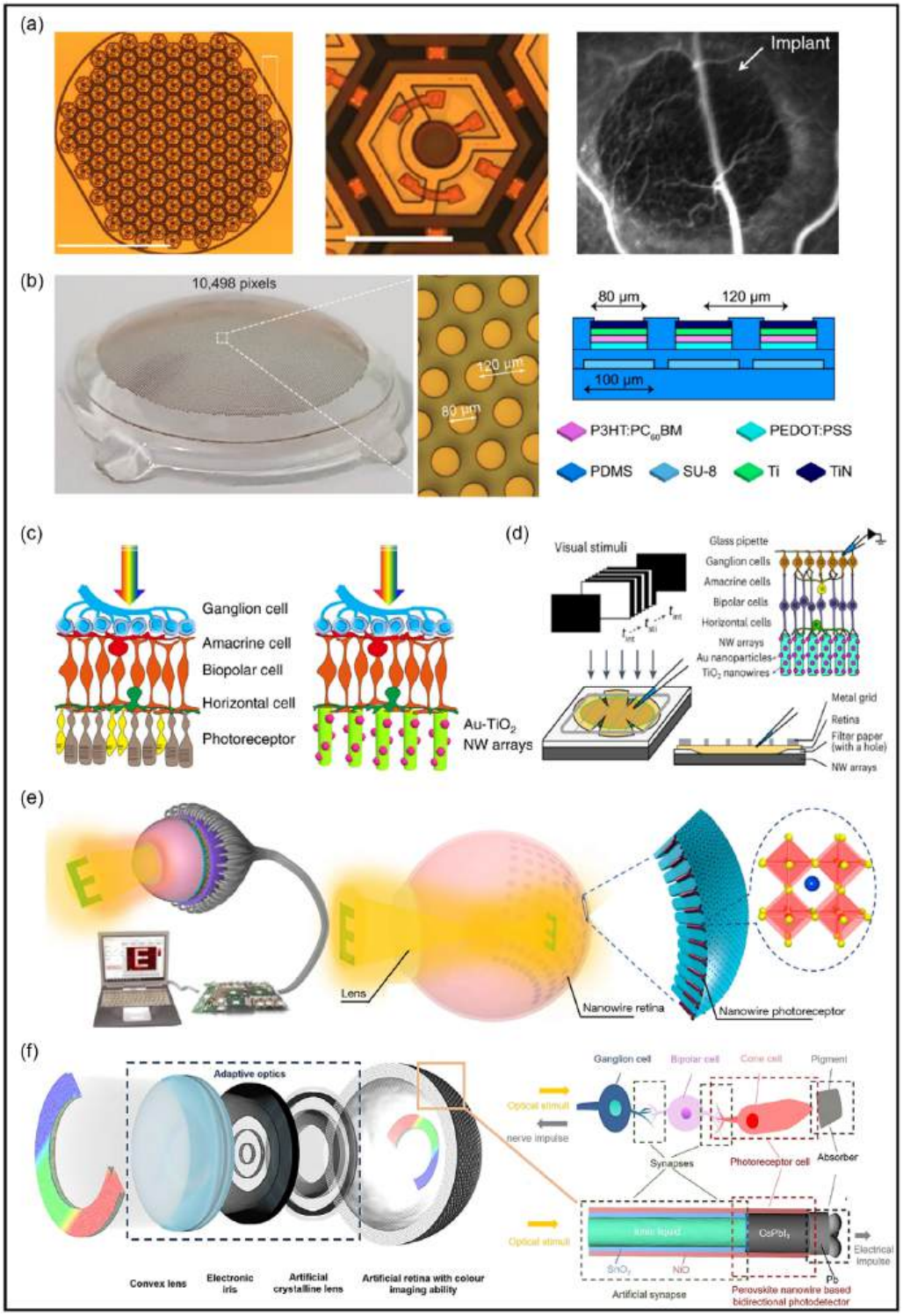

Figure 5. Optoelectronic biointerfaces as retinal prosthesis for vision restoration. a) Silicon-based photovoltaic array and its implantation for the mouse eyeballs. Reproduced with permission.[87] Copyright 2015, Springer Nature. b) The photovoltaic prosthesis with 10 498 pixels (left) and its sketch of the cross-section structure (right). Reproduced with permission.[88] Copyright 2021, Springer Nature. c) Comparison of a retina and NW arrays-interfaced blind retina that lacks photoreceptors. The necrotic photoreceptor layer in the blind retina is replaced by an Au-TiO_2 nanowires array as artificial photoreceptors. Reproduced under terms of the CC-BY license.[89] Copyright 2018, The Authors, Springer Nature. d) Schematic of patch-clamp recording of retinal ganglion cells in blind mice with nanowires arrays attached. Reproduced with permission.[90] Copyright 2024, Springer Nature. e) Schematic of the spherical biomimetic electrochemical eye imaging system. Reproduced with permission.[92] Copyright 2020, Springer Nature. f) Retina neurons and the neuromorphic bionic eye with filter-free color vision. Reproduced under terms of the CC-BY license.[93] Copyright 2023, The Authors, Springer Nature.

(smallest resolvable light spot) and long-term stability, the device offers an optimized platform for the clinical translation of retinal prostheses.[89] Building on these results, the newly fabricated nanowire arrays by Yang et al. showed markedly enhanced photoresponsivity with average photocurrents of ≈13 000 (375 nm), ≈1300 (470 nm), and ≈1100 pA (546 nm) under comparable illumination intensities. In blind mouse models, these devices achieved significant functional restoration, demonstrating a spatial resolution of 77.5 μm and restored visual acuity of 0.3–0.4 cycles per degree, thereby successfully recovering light perception capabilities (Figure 5d).[90] In very recently, they developed a next-generation retinal nanoprosthesis based on tellurium nanowire networks, which intrinsically convert broadband light (from visible to infrared) into electrical signals through efficient photovoltaic conversion, generating large photocurrents under zero external bias without requiring additional auxiliary equipment.[91] Beyond titanium dioxide and tellurium nanowire arrays, recent research on chalcogenide nanowire arrays in the bionic eye has also made significant progress. Gu et al. pioneered an electrochemical bionic eye featuring a hemispherical perovskite ($FAPbI_3$) nanowire array (4.6×10^8 cm^{-2} density) grown on porous alumina via vapor deposition process (Figure 5e).[92] The nanowire array generated a photocurrent of 0.3 nA under weak illumination of 0.3 μW cm^{-2}, with a responsivity of up to 303.2 mA W^{-1}. Liquid metal interconnects enabled nanoscale addressing, delivering rapid photoresponse, high responsivity, and ultralow-light sensitivity across a wide field-of-view with preliminary grayscale image reconstruction capability. This study achieved a functional upgrade from the work of Long et al. by developing a neuromorphic retina of fully inorganic $CsPbI_3$ nanowire arrays composite with SnO_2/NiO

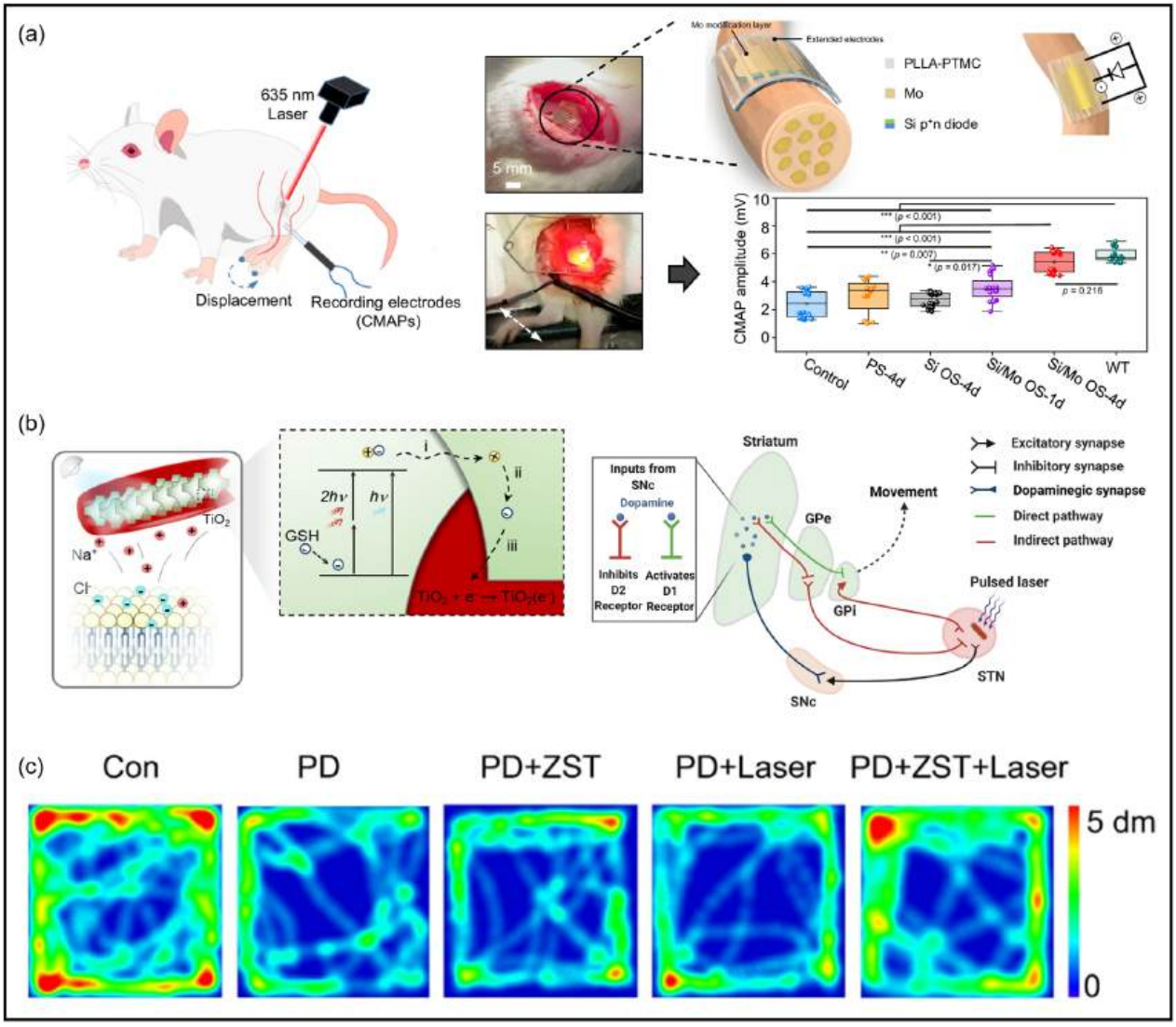

Figure 6. Optoelectronic biointerfaces for neural therapeutics. a) A biodegradable and flexible neural interface for optoelectronic stimulation of peripheral nerves to promote its regeneration. The CMAP amplitude of mouse at 8 weeks postoperatively. Reproduced with permission.[95] Copyright 2024, Springer Nature. b) Non-Faradaic capacitive mechanism of ZST-mediated optoelectrical modulation for therapeutic intervention in a mouse model of Parkinson's disease. c) Representative locomotor trajectories of mice from Con, PD, PD + ZST, PD + Laser, and PD + ZST + Laser groups. Reproduced under terms of the CC-BY license.[96] Copyright 2024, The Authors, Springer Nature.

(tin dioxide/nickel oxide) core-shell nanotubes, as shown in Figure 5f.[93] Under illumination at 650 nm (4.88 mW cm^{-2}), 520 nm (4.93 mW cm^{-2}), and 405 nm (6.59 mW cm^{-2}), the device generated photocurrent densities of ≈2.5, 4.0, and 6.0 μA cm^{-2}, respectively. The wavelength-dependent bidirectional synaptic photoresponse mechanism modulated by ionic liquids allows filter-free color visual recognition at zero bias and full-color image reconstruction. This is achieved by exploiting the polarity difference between the negative photocurrent induced by red/green light and the positive response to blue light, together with bias-modulated color selectivity.

Despite progress, retinal prostheses based on optoelectronic biointerfaces still face challenges: 1) material stability in physiological conditions, 2) reliable wireless power transfer, 3) precise implantation of high-density electrodes, and 4) adaptive neural interfaces for post-implantation cortical plasticity. To enable effective visual restoration in degenerative retinal diseases, next-generation systems must integrate wireless functionality, dynamic polychromatic vision, and biocompatible energy solutions.

7. Optoelectronic Biointerfaces for Neural Therapeutics

Precision neuromodulation has become a pivotal area in modern medicine, given that neurological dysfunction underlies a broad spectrum of disorders.[94] Recent advances in optoelectronic modulation devices—featuring implantable, minimally invasive systems with high spatial and temporal resolution—offer transformative potential for biomedical applications, including nerve repair and disease intervention.

The development of biodegradable optoelectronic devices represents a paradigm shift in peripheral nerve repair. Sun et al. engineered a silicon-/molybdenum-based bioresorbable neural interface that mediates transdermal photostimulation under 635 nm red light (**Figure 6**a).[95] In a rabbit facial nerve injury model, the photogenerated current (≈35 nA, ≈0.1 nC at 0.95 W cm^{-2} illumination) from this device accelerated axonal regeneration and promoted remyelination. Notably, the device's self-degradation profile—complete absorption within 6 weeks post-implantation—could eliminate secondary surgical extraction, establishing a "implant-stimulate-vanish" therapeutic paradigm for traumatic neuropathies. For disorders requiring deep-tissue neuromodulation, Chen et al. developed a design of zinc porphyrin supramolecular nanorod coated by TiO_2 (ZST). This system employed non-Faradaic (capacitive) charge injection activated by far-field femtosecond laser irradiation, achieving 2 mm penetration depth in brain tissue, as shown in Figure 6b.[96] Under 532 nm illumination, ZST generated currents exceeding 200 pA at a power density of 13.5 mW cm^{-2}. Increasing the pulse duration from 0.5 to 1.5 ms produced only subthreshold depolarizations, whereas an action potential was elicited either at 2.0 ms (27.0 μJ cm^{-2}) or at 1.0 ms when the power density reached 23.5 mW cm^{-2}. In a Parkinsonian murine model, chronic ZST-mediated neuromodulation restored motor function while preserving dopaminergic neuron viability in the substantia nigra pars compacta, demonstrating dual therapeutic and neuroprotective efficacy, as shown in Figure 6c. However, current brain modulation devices still need additional optimization in terms of performance metrics, material degradation characteristics, and light penetration efficacy. The use of photoelectronic biointerfaces in neural tissue repair and treatment of neurological disorders remains relatively underexplored, with ongoing efforts focused on expanding their biomedical applications.[97,98]

8. Conclusion and Outlook

This paper reviews the latest developments in wireless, implantable optoelectronic interfaces for nongenetic neural modulation and therapeutics, focusing on photo-responsive systems that combine biocompatible materials with advanced engineering to achieve minimally invasive, spatiotemporally precise stimulation of neural and tissue activity. By converting programmed light inputs into electrical signals, they support targeted modulations ranging from single cells to entire organs. This platform shows promise for clinical applications in epilepsy, Parkinson's disease, and visual impairment, while reducing ethical concerns. Notwithstanding recent progresses, several key technical and translational challenges are yet to be resolved.

First, poor optoelectronic conversion efficiency of existing materials and attenuation of light as it propagates through biological tissue, both of which greatly constrain stimulation efficacy. As a result, high-power light sources are often required to achieve adequate electrical output. Such high-intensity illumination increases the risk of thermal damage due to localized heating. This challenge is amplified in deep-tissue applications, where photon scattering and absorption by intervening tissues reduce optical energy delivery, further compromising the reliability and uniformity of optoelectronic stimulation.[99] Another key issue is ensuring precise alignment of external light sources with implanted optoelectronic devices, particularly in freely moving subjects where body motion can disrupt light delivery. Solving this issue demands strategies for motion compensation, dynamic beam steering, or the integration of autonomous, body-conformal light delivery systems that maintain optical coupling under real-world biomedical scenarios.

Second, although the operational principles of optoelectronic biointerfaces have been discussed previously, a deeper and quantitatively defined mechanistic understanding is still incomplete—particularly in distinguishing the functional outcomes of suprathreshold and subthreshold stimulation. Most existing platforms operate in the suprathreshold regime, generating sufficient photogenerated current to depolarize membranes and evoke action potentials. Deep brain stimulation and cochlear implants are examples of this method that provide effective and localized stimulation. They stop bad activity or restore function by activating high-frequency signals.[100–102] However, suprathreshold stimulation lacks the precision required for highly selective or sustained neuromodulation. In contrast, subthreshold stimulation modulates neuronal excitability and network dynamics without eliciting action potentials. This makes it possible to use more subtle and long-lasting treatments.[103] Subthreshold methods keep spatial specificity while using less power and reducing neural fatigue, as shown by applications like retinal prosthetics and transcutaneous vagus nerve

stimulation.[104,105] While offering these advantages, subthreshold strategies are still underdeveloped in optoelectronic systems for neurological therapeutics. Bridging this gap needs advances in circuit design and closed-loop control to realize real-time, adaptive neuromodulation. Such progress could pave the way for more personalized therapies across a wide range of neurological disorders.[106]

Finally, future study should focus on constructing standardized and comparable evaluation methodologies. It is difficult to evaluate the optoelectronic performances of various biointerfaces introduced in this review, owing to lacking of a unified standard test method. Meanwhile, because of the inherent complexity and tissue-specific properties of light propagation, the actual electrical stimulation generated by an implanted device cannot be precisely quantified. Consequently, even for the same device, its photoelectric response and modulation effects under in vitro and in vivo conditions often show limited correspondence. Since accurate electrical stimulation is fundamental to effective neural modulation, the relationship between light intensity, stimulation strength, and efficacy should be thoroughly evaluated under both in vivo and in vitro conditions. The fundamental mechanisms underlying optoelectronic neuromodulation closely parallel those of well-established electrode-based neurostimulation. Therefore, further evaluations should prioritize quantitative, systematic comparisons between optoelectronic and conventional electrical stimulation paradigms. Such comparisons require careful alignment of stimulation parameters, including target sites, energy delivery, charge density, pulse frequency, and readout metrics (e.g., evoked potentials, calcium dynamics, or behavioral responses). Establishing this benchmark framework will not only facilitate cross-study comparisons, but also accelerate clinical translation by providing clear, reproducible therapeutic efficacy metrics.[107,108]

In summary, ongoing multidisciplinary research efforts are expected to systematically address these multifaceted challenges. By integrating advances in the development of biocompatible materials, precise neuromodulation techniques, and closed-loop bioelectronic systems that combine real-time neural sensing with adaptive stimulation, these collaborative initiatives could lay the groundwork for a new generation of targeted, patient-specific therapies for various neurological disorders.

Acknowledgements

This work was supported by Tsinghua-Toyota Joint Research Fund (to X.S.); the National Natural Science Foundation of China (NSFC, nos. T2425003 and 52272277 to X.S.; no. 62435016 to H.W.); the Basic and Applied Basic Research Foundation of Guangdong Province (no. 2025A1515010752 to H.W.).

Conflict of Interest

The authors declare no conflict of interest.

Keywords

neuromodulation, nongenetic, optoelectronic biointerfaces, semiconductors, therapeutics, wireless

Received: June 16, 2025
Revised: August 19, 2025
Published online: September 27, 2025

[1] H. Chiel, R. Beer, *Trends Neurosci.* **1997**, *20*, 553.
[2] A. Fontanini, D. Katz, *J. Neurophysiol.* **2008**, *100*, 1160.
[3] R. Yuste, *Nat. Rev. Neurosci.* **2015**, *16*, 487.
[4] V. Feigin, T. Vos, E. Nichols, M. Owolabi, W. Carroll, M. Dichgans, G. Deuschl, P. Parmar, M. Brainin, C. Murray, *Lancet Neurol.* **2020**, *19*, 255.
[5] W. Zahra, S. Rai, H. Birla, S. Singh, H. Dilnashin, A. Rathore, S. Singh, *Bioecon. Sustain. Dev.* **2019**, 333.
[6] G. Balbinot, M. Milosevic, C. Morshead, S. Iwasa, J. Zariffa, L. Milosevic, T. Valiante, J. Hoffer, M. Popovic, *J. Physiol.* **2025**, *603*, 247.
[7] D. Brocker, W. Grill, *Handb. Clin. Neurol.* **2013**, *116*, 3.
[8] J. Newton, S. Knisley, X. Zhou, A. Pollard, R. Ideker, *J. Cardiovasc. Electrophysiol.* **1999**, *10*, 234.
[9] F. Rattay, *Neuroscience* **1999**, *89*, 335.
[10] D. Merrill, M. Bikson, J. Jefferys, *J. Neurosci. Methods* **2005**, *141*, 171.
[11] K. Lindberg, E. Dougherty, *Front. Comput. Neurosci.* **2019**, *13*, 17.
[12] M. Stefano, F. Cordella, A. Loppini, S. Filippi, L. Zollo, *IEEE Trans. Neural Syst. Rehab. Eng.* **2021**, *29*, 397.
[13] P. Werginz, S. Fried, F. Rattay, *Neuroscience* **2014**, *266*, 162.
[14] J. Huang, Z. Ye, X. Hu, L. Lu, Z. Luo, *Glia* **2010**, *58*, 622.
[15] X. Yan, J. Liu, J. Huang, M. Huang, F. He, Z. Ye, W. Xiao, X. Hu, Z. Luo, *Neurochem. Res.* **2014**, *39*, 129.
[16] A. Lozano, J. Dostrovsky, R. Chen, P. Ashby, *Lancet Neurol.* **2002**, *1*, 225.
[17] P. Limousin, P. Krack, P. Pollak, A. Benazzouz, C. Ardouin, D. Hoffmann, A. Benabid, *N. Engl. J. Med.* **1998**, *339*, 1105.
[18] H. Knotkova, C. Hamani, E. Sivanesan, M. Le Beuffe, J. Moon, S. Cohen, M. Huntoon, *Lancet* **2021**, *397*, 2111.
[19] M. Johnson, C. Paley, G. Jones, M. Mulvey, P. Wittkopf, *BMJ Open* **2022**, *12*, e051073.
[20] P. Boon, R. Raedt, V. Herdt, T. Wyckhuys, K. Vonck, *Neurotherapeutics* **2009**, *6*, 218.
[21] A. Berényi, M. Belluscio, D. Mao, G. Buzsáki, *Science* **2012**, *337*, 735.
[22] K. Song, J. Han, T. Lim, N. Kim, S. Shin, J. Kim, H. Choo, S. Jeong, Y. Kim, Z. Wang, J. Lee, *Adv. Healthc. Mater.* **2016**, *5*, 1572.
[23] M. Sohail, D. Uslan, A. Khan, P. Friedman, D. Hayes, W. Wilson, J. Steckelberg, S. Stoner, L. Baddour, *J. Am. Coll. Cardiol.* **2007**, *49*, 1851.
[24] C. Rooden, S. Molhoek, F. Rosendaal, M. Schalij, A. Meinders, M. Huisman, *J. Cardiovasc. Electrophysiol.* **2004**, *15*, 1258.
[25] R. Hauser, D. Hayes, L. Kallinen, D. Cannom, A. Epstein, A. Almquist, S. Song, G. Tyers, S. Vlay, M. Irwin, *Heart Rhythm* **2007**, *4*, 154.
[26] E. Buch, N. Boyle, P. Belott, *Circulation* **2011**, *123*, E378.
[27] C. McLeod, C. Jost, C. Warnes, D. Hodge, L. Hyberger, H. Connolly, S. Asirvatham, J. Dearani, D. Hayes, N. Ammash, *J. Interv. Card. Electrophysiol.* **2010**, *28*, 235.
[28] M. Wildbolz, H. Dave, R. Weber, M. Gass, C. Balmer, *Pediatr. Cardiol.* **2020**, *41*, 910.
[29] L. Vos, J. Kammeraad, M. Freund, A. Blank, J. Breur, *Europace* **2017**, *19*, 581.
[30] L. Wang, T. Zhang, J. Lei, S. Wang, Y. Guan, K. Chen, C. Li, Y. Song, W. Li, S. Wang, Z. Jia, S. Chen, J. Bai, B. Yu, C. Yang, P. Sun, Q. Wang, X. Sheng, J. Peng, Y. Fan, L. Wang, M. Zhang, Y. Wang, L. Yin, *Nat. Commun.* **2025**, *16*, 1716.
[31] P. Meredith, C. Bettinger, M. Irimia-Vladu, A. Mostert, P. Schwenn, *Rep. Prog. Phys.* **2013**, *76*, 034501.
[32] Y. Jiang, B. Tian, *Nat. Rev. Mater.* **2018**, *3*, 473.

[33] H. Xu, L. Yin, C. Liu, X. Sheng, N. Zhao, *Adv. Mater.* **2018**, *30*, 1800156.
[34] N. Thanjavur, L. Bugude, Y. Kim, *Biosensors* **2025**, *15*, 38.
[35] H. Wang, P. Sun, L. Yin, X. Sheng, *InfoMat* **2020**, *2*, 527.
[36] H. Wang, J. Tian, Y. Jiang, S. Liu, J. Zheng, N. Li, G. Wang, F. Dong, J. Chen, Y. Xie, Y. Huang, X. Cai, X. Wang, W. Xiong, H. Qi, L. Yin, Y. Wang, X. Sheng, *Sci. Adv.* **2023**, *9*, eabq7750.
[37] W. Zhi, Y. Li, L. Wang, X. Hu, *Cells* **2025**, *14*, 122.
[38] V. Emiliani, E. Entcheva, R. Hedrich, P. Hegemann, K. Konrad, C. Lüscher, M. Mahn, Z. Pan, R. Sims, J. Vierock, O. Yizhar, *Nat. Rev. Methods Primers* **2022**, *2*, 55.
[39] L. Fenno, O. Yizhar, K. Deisseroth, *Annu. Rev. Neurosci.* **2011**, *34*, 389.
[40] A. Guru, R. Post, Y. Ho, M. Warden, *Int. J. Neuropsychopharmacol.* **2015**, *18*, pyv079.
[41] J. Shi, P. Li, S. Kim, B. Tian, *Nat. Rev. Bioeng.* **2025**, *3*, 485.
[42] M. Han, O. Karatum, S. Nizamoglu, *ACS Appl. Mater. Interfaces* **2022**, *14*, 20468.
[43] C. Yang, Z. Cheng, P. Li, B. Tian, *Acc. Chem. Res.* **2024**, *57*, 1398.
[44] O. Karatum, M. Gwak, J. Hyun, A. Onal, G. Koirala, T. Kim, S. Nizamoglu, *Chem. Soc. Rev.* **2023**, *52*, 3326.
[45] Y. Huang, K. Yao, Q. Zhang, X. Huang, Z. Chen, Y. Zhou, X. Yu, *Chem. Soc. Rev.* **2024**, *53*, 8632.
[46] A. Harris, C. Newbold, P. Carter, R. Cowan, G. Wallace, *J. Neural Eng.* **2018**, *15*, 046015.
[47] M. Walter, E. Warren, J. McKone, S. Boettcher, Q. Mi, E. Santori, N. Lewis, *Chem. Rev.* **2010**, *110*, 6446.
[48] M. Mayer, *Curr. Opin. Electrochem.* **2017**, *2*, 104.
[49] Y. Jiang, X. Li, B. Liu, J. Yi, Y. Fang, F. Shi, X. Gao, E. Sudzilovsky, R. Parameswaran, K. Koehler, V. Nair, J. Yue, K. Guo, H. Tsai, G. Freyermuth, R. Wong, C. Kao, C. Chen, A. Nicholls, X. Wu, G. Shepherd, B. Tian, *Nat. Biomed. Eng.* **2018**, *2*, 508.
[50] J. Ehlich, C. Vasícek, J. Dobes, A. Ruggiero, M. Vejvodová, E. Glowacki, *ACS Appl. Mater. Interfaces* **2024**, *16*, 53567.
[51] A. Hung, D. Zhou, R. Greenberg, I. Goldberg, J. Judy, *J. Electrochem. Soc.* **2007**, *154*, C479.
[52] D. Brandman, T. Hosman, J. Saab, M. Burkhart, B. Shanahan, J. Ciancibello, A. Sarma, D. Milstein, C. Vargas-Irwin, B. Franco, J. Kelemen, C. Blabe, B. Murphy, D. R. Young, F. Willett, C. Pandarinath, S. Stavisky, R. F. Kirsch, B. Walter, A. Ajiboye, S. Cash, E. Eskandar, J. Miller, J. Sweet, K. Shenoy, J. Henderson, B. Jarosiewicz, M. Harrison, J. Simeral, L. Hochberg, *J. Neural Eng.* **2018**, *15*, 026007.
[53] Y. Jiang, R. Parameswaran, X. Li, J. Carvalho-de-Souza, X. Gao, L. Meng, F. Bezanilla, G. Shepherd, B. Tian, *Nat. Protoc.* **2019**, *14*, 1339.
[54] A. Alabugin, *Photochem. Photobiol.* **2019**, *95*, 722.
[55] S. Golovynskyi, I. Golovynska, L. Stepanova, O. Datsenko, L. Liu, J. Qu, T. Ohulchanskyy, *J. Biophotonics* **2018**, *11*, 201800141.
[56] A. Bozkurt, B. Onaral, *Biomed. Eng. Online* **2004**, *3*, 9.
[57] R. Matthes, *Health Phys.* **2020**, *118*, 580.
[58] E. Song, J. Li, S. Won, W. Bai, J. Rogers, *Nat. Mater.* **2020**, *19*, 590.
[59] M. Brini, T. Calì, D. Ottolini, E. Carafoli, *Cell. Mol. Life Sci.* **2014**, *71*, 2787.
[60] J. Zhang, *Arxiv* **2019**, 1906.01703.
[61] Y. Gao, Y. Guo, Y. Yang, Y. Tang, B. Wang, Q. Yan, X. Chen, J. Cai, L. Fang, Z. Xiong, F. Gao, C. Wu, J. Wang, J. Tang, L. Shi, D. Li, *Adv. Mater.* **2024**, *36*, 2305632.
[62] Y. Huang, Y. Cui, H. Deng, J. Wang, R. Hong, S. Hu, H. Hou, Y. Dong, H. Wang, J. Chen, L. Li, Y. Xie, P. Sun, X. Fu, L. Yin, W. Xiong, S. Shi, M. Luo, S. Wang, X. Li, X. Sheng, *Nat. Biomed. Eng.* **2023**, *7*, 486.
[63] O. Karatum, H. Kaleli, G. Eren, A. Sahin, S. Nizamoglu, *ACS Nano* **2022**, *16*, 8233.
[64] R. Balamur, T. Kaya, S. Sariyer, H. Kaleli, A. Onal, U. Caliskan, M. Hasanreisoglu, R. Demir-Cakan, S. Nizamoglu, *Adv. Funct. Mater.* **2025**, *35*, 2422083.
[65] M. Jakesová, M. Ejneby, V. Derek, T. Schmidt, M. Gryszel, J. Brask, R. Schindl, D. Simon, M. Berggren, F. Elinder, E. Glowacki, *Sci. Adv.* **2019**, *5*, eaav5265.
[66] D. Rand, M. Jakesová, G. Lubin, I. Vebraite, M. David-Pur, V. Derek, T. Cramer, N. Sariciftci, Y. Hanein, E. Glowacki, *Adv. Mater.* **2018**, *30*, 1707292.
[67] O. Sultana, M. Bandaru, M. Islam, P. Reddy, *Ageing Res. Rev.* **2024**, *100*, 102414.
[68] G. Leisman, A. Moustafa, T. Shafir, *Front. Public Health* **2016**, *4*, 179575.
[69] B. Faw, *Conscious. Cogn.* **2003**, *12*, 83.
[70] F. Missey, B. Botzanowski, L. Migliaccio, E. Acerbo, E. Glowacki, A. Williamson, *J. Neural Eng.* **2021**, *18*, 066016.
[71] M. Nowakowska, M. Jakesová, T. Schmidt, A. Opancar, M. Polz, R. Reimer, J. Fuchs, S. Patz, D. Ziesel, S. Scheruebel, K. Kornmueller, T. Rienmüller, V. Derek, E. Glowacki, R. Schindl, M. Üçal, *Adv. Healthc. Mater.* **2024**, *13*, 2401303.
[72] M. Catala, N. Kubis, *Handb. Clin. Neurol.* **2013**, *115*, 29.
[73] M. Ottayiani, V. Macefield, *Compr. Physiol.* **2022**, *12*, 3989.
[74] S. Prescott, S. Liberles, *Neuron* **2022**, *110*, 579.
[75] S. Breit, A. Kupferberg, G. Rogler, G. Hasler, *Front. Psychiatry* **2018**, *9*, 298797.
[76] M. Stanton-Hicks, J. Salamon, *J. Clin. Neurophysiol.* **1997**, *14*, 46.
[77] X. Chu, X. Song, Q. Li, Y. Li, F. He, X. Gu, D. Ming, *Neural Regen. Res.* **2022**, *17*, 2185.
[78] L. Ni, Z. Yao, Y. Zhao, T. Zhang, J. Wang, S. Li, Z. Chen, *Front. Neurol.* **2023**, *14*, 1081458.
[79] I. Garamendi-Ruiz, J. Gómez-Esteban, *Clin. Auton. Res.* **2019**, *29*, 183.
[80] V. Dusi, G. Ferrari, *Herz* **2021**, *46*, 541.
[81] A. Prominski, J. Shi, P. Li, J. Yue, Y. Lin, J. Park, B. Tian, M. Rotenberg, *Nat. Mater.* **2022**, *21*, 647.
[82] M. Ejneby, M. Jakesová, J. Ferrero, L. Migliaccio, I. Sahalianov, Z. Zhao, M. Berggren, D. Khodagholy, V. Derek, J. Gelinas, E. Glowacki, *Nat. Biomed. Eng.* **2022**, *6*, 741.
[83] M. Donahue, M. Ejneby, M. Jakesová, A. Caravaca, G. Andersson, I. Sahalianov, V. Derek, H. Hult, P. Olofsson, E. Glowacki, *J. Neural Eng.* **2022**, *19*, 066031.
[84] M. Jakesová, O. Kunovsky, I. Gablech, D. Khodagholy, J. Gelinas, E. Glowacki, *J. Neural Eng.* **2024**, *21*, 046003.
[85] K. Wert, J. Lin, S. Tsang, *Dev. Ophthalmol.* **2014**, *53*, 33.
[86] H. Scholl, R. Strauss, M. Singh, D. Dalkara, B. Roska, S. Picaud, J. Sahel, *Sci. Transl. Med.* **2016**, *8*, 368rv6-368rv6.
[87] H. Lorach, G. Goetz, R. Smith, X. Lei, Y. Mandel, T. Kamins, K. Mathieson, P. Huie, J. Harris, A. Sher, D. Palanker, *Nat. Med.* **2015**, *21*, 476.
[88] N. Chenais, M. Leccardi, D. Ghezzi, *Commun. Mater.* **2021**, *2*, 28.
[89] J. Tang, N. Qin, Y. Chong, Y. Diao, Yiliguma, Z. Wang, T. Xue, M. Jiang, J. Zhang, G. Zheng, *Nat. Commun.* **2018**, *9*, 786.
[90] R. Yang, P. Zhao, L. Wang, C. Feng, C. Peng, Z. Wang, Y. Zhang, M. Shen, K. Shi, S. Weng, C. Dong, F. Zeng, T. Zhang, X. Chen, S. Wang, Y. Wang, Y. Luo, Q. Chen, Y. Chen, C. Jiang, S. Jia, Z. Yu, J. Liu, F. Wang, S. Jiang, W. Xu, L. Li, G. Wang, X. Mo, G. Zheng, et al., *Nat. Biomed. Eng.* **2024**, *8*, 1018.
[91] S. Wang, C. Jiang, Y. Yu, Z. Zhang, R. Quhe, R. Yang, Y. Tian, X. Chen, W. Fan, Y. Niu, B. Yan, C. Jiang, Y. Wang, Z. Wang, C. Liu, W. Hu, J. Zhang, P. Zhou, *Science* **2025**, *388*, eadu2987.
[92] L. Gu, S. Poddar, Y. Lin, Z. Long, D. Zhang, Q. Zhang, L. Shu, X. Qiu, M. Kam, A. Javey, Z. Fan, *Nature* **2020**, *581*, 278.
[93] Z. Long, X. Qiu, C. Chan, Z. Sun, Z. Yuan, S. Poddar, Y. Zhang, Y. Ding, L. Gu, Y. Zhou, W. Tang, A. Srivastava, C. X. Zou, G. Shen, Z. Fan, *Nat. Commun.* **2023**, *14*, 1972.
[94] B. Haider, J. Oertzen, *Best Pract. Res. Clin. Obstet. Gynaecol.* **2013**, *27*, 867.

[95] P. Sun, C. Li, C. Yang, M. Sun, H. Hou, Y. Guan, J. Chen, S. Liu, K. Chen, Y. Ma, Y. Huang, X. Li, H. Wang, L. Wang, S. Chen, H. Cheng, W. Xiong, X. Sheng, M. Zhang, J. Peng, S. Wang, Y. Wang, L. Yin, *Nat. Commun.* **2024**, *15*, 4721.
[96] J. Chen, Y. Liu, F. Chen, M. Guo, J. Zhou, P. Fu, X. Zhang, X. Wang, H. Wang, W. Hua, J. Chen, J. Hu, Y. Mao, D. Jin, W. Bu, *Nat. Commun.* **2024**, *15*, 405.
[97] P. Li, J. Zhang, H. Hayashi, J. Yue, W. Li, C. Yang, C. Sun, J. Shi, J. Huberman-Shlaes, N. Hibino, B. Tian, *Nature* **2024**, *631*, 990.
[98] Y. Zhang, E. Rytkin, L. Zeng, J. Kim, L. Tang, H. Zhang, A. Mikhailov, K. Zhao, Y. Wang, L. Ding, X. Lu, A. Lantsova, E. Aprea, G. Jiang, S. Li, S. Seo, T. Wang, J. Wang, J. Liu, J. Gu, F. Liu, K. Bailey, Y. Li, A. Burrell, A. Pfenniger, A. Ardashev, T. Yang, N. Liu, Z. Lv, N. Purwanto, et al., *Nature* **2025**, *640*, 77.
[99] S. Jiang, X. Wu, J. Rommelfanger, Z. Ou, S. Hong, *Natl. Sci. Rev.* **2022**, *9*, nwac007.
[100] A. Farokhniaee, M. Lowery, *J. Neural Eng.* **2021**, *18*, 056006.
[101] S. Santaniello, M. McCarthy, E. Montgomery, J. Gale, N. Kopell, S. Sarma, *Proc. Natl. Acad. Sci. USA* **2015**, *112*, E586.
[102] J. Wang, J. Puel, *Physiol. Rev.* **2018**, *98*, 2477.
[103] O. Amsalem, H. Inagaki, J. Yu, K. Svoboda, R. Darshan, *Nat. Commun.* **2024**, *15*, 7958.
[104] S. Sekhar, A. Jalligampala, E. Zrenner, D. Rathbun, *J. Neural Eng.* **2016**, *13*, 046004.
[105] F. Capone, G. Assenza, G.i Pino, G. Musumeci, F. Ranieri, L. Florio, C. Barbato, V. Lazzaro, *J. Neural Transm.* **2015**, *122*, 679.
[106] T. Radman, R. Ramos, J. Brumberg, M. Bikson, *Brain Stimul.* **2009**, *2*, 215.
[107] A. Indahlastari, M. Chauhan, R. Sadleir, *J. Neural Eng.* **2019**, *16*, 026019.
[108] C. Boehler, S. Carli, L. Fadiga, T. Stieglitz, M. Asplund, *Nat. Protoc.* **2020**, *15*, 3557.
[109] W. Chung, J. Jang, G. Cui, S. Lee, H. Jeong, H. Kang, H. Seo, S. Kim, E. Kim, J. Lee, S. Lee, S. Byeon, J. Park, *Nat. Nanotechnol.* **2024**, *19*, 688.
[110] R. Parameswaran, J. Carvalho-de-Souza, Y. Jiang, M. Burke, J. Zimmerman, K. Koehler, A. Phillips, J. Yi, E. Adams, F. Bezanilla, B. Tian, *Nat. Nanotechnol.* **2018**, *13*, 260.
[111] A. Thalhammer, M. Fontanini, J. Shi, D. Scaini, L. Recupero, A. Evtushenko, Y. Fu, S. Pavagada, A. Bistrovic-Popov, L. Fruk, B. Tian, L. Ballerini, *Sci. Adv.* **2022**, *8*, eqbp9257.
[112] X. Fu, Z. Hu, W. Li, L. Ma, J. Chen, M. Liu, J. Liu, S. Hu, H. Wang, Y. Huang, G. Tang, B. Zhang, X. Cai, Y. Wang, L. Li, J. Ma, S. Shi, L. Yin, H. Zhang, X. Li, X. Sheng, *Proc. Natl. Acad. Sci. USA* **2024**, *121*, e2404164121.
[113] K. Mathieson, J. Loudin, G. Goetz, P. Huie, L. Wang, T. Kamins, L. Galambos, R. Smith, J. Harris, A. Sher, D. Palanker, *Nat. Photonics* **2012**, *6*, 391.
[114] P. Prévot, K. Gehere, F. Arcizet, H. Akolkar, M. Khoei, K. Blaize, O. Oubari, P. Daye, M. Lanoë, M. Valet, S. Dalouz, P. Langlois, E. Esposito, V. Forster, E. Dubus, N. Wattiez, E. Brazhnikova, C. Nouvel-Jaillard, Y. LeMer, J. Demilly, C. Fovet, P. Hantraye, M. Weissenburger, H. Lorach, E. Bouillet, M. Deterre, R. Hornig, G. Buc, J. Sahel, G. Chenegros, et al., *Nat. Biomed. Eng.* **2020**, *4*, 172.
[115] T. Pappas, W. Wickramanyake, E. Jan, M. Motamedi, M. Brodwick, N. Kotov, *Nano Lett.* **2007**, *7*, 513.
[116] K. Lugo, X. Miao, F. Rieke, L. Lin, *Biomed. Opt. Express* **2012**, *3*, 447.
[117] H. Jalali, M. Aria, U. Dikbas, S. Sadeghi, B. Kumar, M. Sahin, I. Kavakli, C. Owang, S. Nizamoglu, *ACS Nano* **2018**, *12*, 8104.
[118] H. Jalali, O. Karatum, R. Melikov, U. Dikbas, S. Sadeghi, E. Yildiz, I. Dogru, G. Eren, C. Ergun, A. Sahin, I. Kavakli, S. Nizamoglu, *Nano Lett.* **2019**, *19*, 5975.
[119] O. Karatum, G. Eren, R. Melikov, A. Onal, C. OwYang, M. Sahin, S. Nizamoglu, *Sci. Rep.* **2021**, *11*, 2460.
[120] M. Han, H. Jalali, E. Yildiz, M. Qureshi, A. Sahin, S. Nizamoglu, *Commun. Mater.* **2021**, *2*, 19.
[121] O. Karatum, M. Aria, G. Eren, E. Yildiz, R. Melikov, S. Srivastava, S. Surme, I. Dogru, H. Jalali, B. Ulgut, A. Sahin, I. Kavakli, S. Nizamoglu, *Front. Neurosci.* **2021**, *15*, 652608.
[122] R. Balamur, G. Eren, H. Kaleli, O. Karatum, L. Kaya, M. Hasanreisoglu, S. Nizamoglu, *Adv. Sci.* **2024**, *11*, 2401753.
[123] L. Bareket, N. Waiskopf, D. Rand, G. Lubin, M. David-Pur, J. Ben-Dov, S. Roy, C. Eleftheriou, E. Sernagor, O. Cheshnovsky, U. Banin, Y. Hanein, *Nano Lett.* **2014**, *14*, 6685.
[124] Y. Yao, A. Ahnood, A. Chambers, W. Tong, S. Prawer, *Adv. Healthc. Mater.* **2025**, *14*, 2403901.
[125] A. Markov, A. Gerasimenko, A. Boromangnaeva, S. Shashova, E. Iusupovskaia, U. Kurilova, V. Nikitina, I. Suetina, M. Mezentseva, M. Savelyev, P. Timashev, D. Telyshev, X. Liang, *Nano Res.* **2023**, *16*, 5809.
[126] E. Iusupovskaia, A. Gerasimenko, S. Selishchev, D. Telyshev, A. Markov, *Biomed. Eng.* **2024**, *58*, 143.
[127] S. Srivastava, R. Melikov, M. Aria, U. Dikbas, I. Kavakl, S. Nizamoglu, *Phys. Rev. Appl.* **2019**, *11*, 044012.
[128] R. Melikov, S. Srivastava, O. Karatum, I. Dogru-Yuksel, U. Dikbas, I. Kavakli, S. Nizamoglu, *Biomed. Opt. Express* **2020**, *11*, 6068.
[129] S. Srivastava, R. Melikov, E. Yildiz, M. Han, A. Sahin, S. Nizamoglu, *Biomed. Opt. Express* **2020**, *11*, 5237.
[130] M. DiFrancesco, E. Colombo, E. Papaleo, J. Maya-Vetencourt, G. Manfredi, G. Lanzani, F. Benfenati, *Carbon* **2020**, *162*, 308.

Jinglin Ye obtained his bachelor degree from South China Agricultural University in 2023. He is pursuing his master degree under the supervision of Prof. Huachun Wang in the School of Integrated Circuits at Sun Yat-sen University, China. His research interests focus on semiconductor-based optoelectronic devices for biomedical applications.

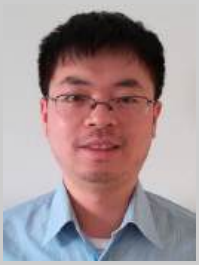

Xing Sheng is currently working as a professor in the Department of Electronic Engineering at Tsinghua University, China. He received his bachelor and Ph.D. degrees from Tsinghua University and Massachusetts Institute of Technology, respectively. His current research is focused on advanced optoelectronic materials, devices, and systems for biomedical applications.

Huachun Wang is currently working as an assistant professor in the School of Integrated Circuits at Sun Yat-sen University, China. He received his Ph.D. degree in electronic science and technology from Tsinghua University. His research focuses on the development of electronic devices and circuits for wireless bioelectronic and biomedical applications.